ISSN 2616-5767 Vol.6, Issue 4: 28-35, DOI: 10.25236/AJETS.2023.060405

Isofilm thickness control of hydrostatic bearings under piezoelectric stacked film restrictors

Zhou Yue[1], Kang Huimin[1,a,*], Zhang Xuewen[2]

[1]*School of Mechanical Engineering, Hunan University of Science and Technology, Xiangtan, China*
[2]*Harbin Electric Corporation Wind Power Co., Ltd, Xiangtan, China*
[a]*bxykanghm@163.com*
[*]*Corresponding author*

Abstract: *In view of the problem of heat accumulation of oil film in heavy-duty hydrostatic bearings, the method of equal oil film thickness control is used to reduce the eccentricity of the spindle and reduce the heat accumulation. Based on the piezoelectric equation, the mathematical model of the piezoelectric stacked thin film flow rattle was obtained. Based on the flow formula of the oil cavity of the throttle and the hydrostatic bearing, the bearing capacity formula of the hydrostatic bearing was obtained. The transfer function of the control system is obtained by linearizing the bearing capacity of the hydrostatic bearing by the regress function in MATLAB, and finally the control of the equal oil film thickness under the PID algorithm is realized. It is found that the increase of oil supply pressure, bearing width and oil chamber size of hydrostatic bearings can reduce the amplitude of oil film thickness, but has almost no effect on the response time of active control. Hydrostatic bearings under the control of equal oil film thickness significantly improve the bearing capacity and stiffness while driving the eccentricity of the spindle to zero. This makes hydrostatic bearings better suited for high precision and heavy duty applications.*

Keywords: *Hydrostatic bearings; Piezoelectric stacked thin film flow restrictor; Iso-oil film thickness control; PID control*

1. Introduction

Hydrostatic bearings are widely used in various precision and ultra-precision machining fields due to their advantages of high stiffness, high slewing accuracy and long life.[1][2] In order to further improve the working accuracy of hydrostatic bearings, the research of hydrostatic bearings under active flow limiters has become a research hotspot in recent years.[3][4][5] Among them, piezoelectric ceramic materials are widely used because of their compact structure, high control accuracy, simple and convenient control, and fast response speed.[4][5]

Active flow throttling technology based on active flow restrictors has been shown to significantly increase the load carrying capacity and stiffness of hydrostatic bearings.[6][7] YANG et al.[6] studied the dynamic characteristics of hydrostatic bearings under electro-hydraulic valves, and found that electro-hydraulic bearings under PID control can significantly improve the dynamic performance of hydrostatic bearings. Hu Can et al.[3] found that hydrostatic bearings under active throttling can effectively reduce the spindle offset and reduce the steady-state rotation error of hydrostatic bearings. Liu Lei, Liu Baoguo et al.[8] studied the distribution of oil film pressure and temperature of deep and shallow cavity dynamic and static pressure bearings through FLUENT, and found that with the increase of eccentricity, the heat of the oil film began to accumulate, and the bearing capacity and temperature rise of the oil film also increased.

In order to reduce the heat accumulation of oil film in heavy-duty hydrostatic bearings, the method of equal oil film thickness control is used to reduce the eccentricity of the spindle and reduce the heat accumulation of the oil film. Using a relatively easy to control piezoelectric stacked thin film flow restrictor as the active flow restrictor, the mathematical model of the flow restrictor is established based on the piezoelectric equation, and then the bearing capacity formula of the hydrostatic bearing is obtained based on the flow formula of the restrictor and the hydrostatic bearing, and then the active control model of the hydrostatic bearing is established. The method of adjusting the voltage difference control throttle gap of the piezoelectric stacked thin film restrictor by PID control algorithm realizes the control of the equal oil film thickness of the hydrostatic bearing. This makes hydrostatic bearings better suited for high precision and heavy duty applications.

2. Piezoelectric stacked membrane flow restrictor

Since the film deformation in the piezoelectric stacked membrane flow restrictor is less affected by the pressure of the oil cavity and the control process is relatively simple, the piezoelectric stacked membrane flow restrictor is selected as the throttle valve of the active hydrostatic bearing, and its structural schematic is shown in Figure 1. When the spindle is displacement due to external load, the sensor detects the displacement signal, and the control system adjusts the throttle gap of the inverter by changing the voltage difference of the piezoelectric ceramic stack in the piezoelectric stacked membrane restrictor. This increases the pressure difference between the oil chamber of the hydrostatic bearing, so that the spindle center returns to the center of the bearing.

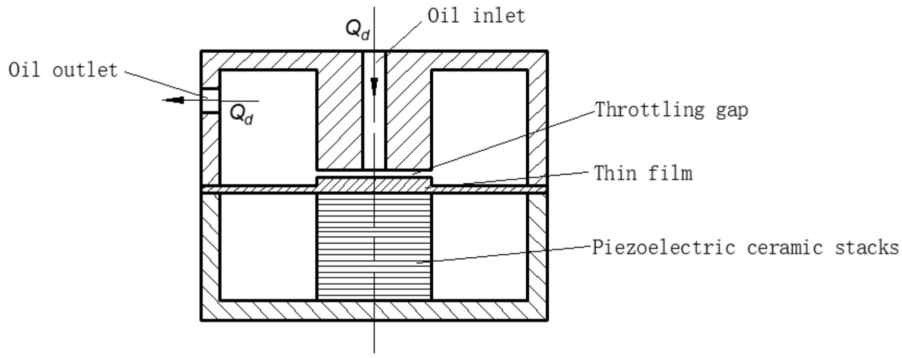

Figure 1: Piezoelectric stacked thin film restrictor schematic

The piezoelectric ceramic in the restrictor is selected from the circular piezoelectric laminated actuator PTY15014401 of a piezoelectric ceramic company in Suzhou, and its parameters are shown in Table 1.[9]

Table 1: Parameters of the round piezoelectric laminated actuator PTY15014401

parameter	numeric value	parameter	numeric value
Piezoelectric ceramic diameter (mm)	Ø14.7	stiffness (N/um)	188
Zero displacement thrust (N@150V)	7500	Piezo height (mm)	40
Standard displacement (um@150V)	40	Rated voltage(V)	150

This round piezo laminated actuator PTY15014401 is made up of stacked piezo ceramic plates, usually directly indicating the height of the actuator. It can be seen from Table 1 that in the case of a voltage difference of 150V across the piezoelectric ceramic pile, when the external pressure is zero, the piezoelectric ceramic pile will elongate by 40um, and when the piezoelectric ceramic pile is in zero displacement, the pressure given to the outside is 7500N, combined with the diameter of the piezoelectric ceramics, the stress of the piezoelectric ceramic is 44191293P_a.

Based on the piezoelectric equation of piezoelectric materials, the displacement D_3 of piezoelectric materials under the joint action of stress T_3 and electric E_3 field can be expressed by the following formula.

$$D_3 = d_{33}T_3 + \varepsilon_{33}E_3 \tag{1}$$

Where d_{33} is the piezoelectric constant, that is, the ratio of the displacement and stress of the piezoelectric material under the action of a certain electric field, and ε_{33} is the dielectric constant when the stress T_3=0 (or T_3 is constant), which is called the free permittivity.

The combination of equation (1) and Table 1 yields a graph of displacement vs. stress at different voltages, as shown in Figure 2.

ISSN 2616-5767 Vol.6, Issue 4: 28-35, DOI: 10.25236/AJETS.2023.060405

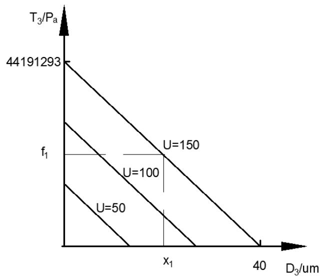

Figure 2: Charge displacement vs. stress plot at different voltages

Figure 2 shows the relationship between stress T_3, displacement D_3 and voltage ΔU.

$$D_3 = \frac{4}{15}\Delta U - \frac{40}{44191293} T_3 \tag{2}$$

Since piezopile elongation is easier relative to compression, piezopile elongation in the thickness direction controls throttle gaps. When the voltage ΔU=75V and T_3=0Pa, the value of the throttle gap is the standard value. If the DC voltage of the piezoelectric ceramic stack is increased, the piezoelectric ceramic stack increases the expansion and contraction, and the throttle gap decreases. If the DC voltage of the piezoelectric ceramic stack is reduced, the piezoelectric ceramic stack reduces the expansion and contraction and the throttling gap increases. Set h_{p0} standard throttle gap for this restrictor. Then the throttle gap h_p (um) of the piezoelectric stacked thin film flow ratifier is calculated as follows.

$$h_p = h_{p0} - \frac{4}{15}(\Delta U - 75) + \frac{40}{44191293} T_3 \tag{3}$$

Since the order of magnitude of the oil supply pressure is 10^6, the stress displacement provided by the oil supply pressure is much smaller than the electrical displacement, so the change of stress displacement is ignored and equation (3) is reduced to the following calculation formula.

$$h_p = h_{p0} - \frac{4}{15}(\Delta U - 75) \tag{4}$$

The flow rate of a piezoelectric stacked type membrane flow restrictor Q_d the same as that of a normal thin film flow restrictor, and its calculation formula is as follows.

$$Q_d = \frac{\pi {h_p}^3 (P_s - P_r)}{6\mu \ln\left(\frac{r_{d2}}{r_{d1}}\right)} \tag{5}$$

In the formula, the P_s and P_r are the oil supply pressure and the oil chamber pressure, and the r_{d1} and r_{d2} are the radius of the oil inlet hole and the radius of the throttle round table of the flow restrictor, respectively.

3. Hydrostatic bearing systems

A schematic diagram of the oil chamber pressure of a hydrostatic bearing is shown in Figure 3.

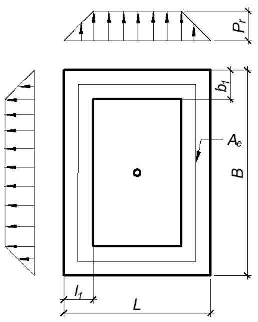

Figure 3: Schematic diagram of oil chamber pressure

The flow rate around the oil chamber in a hydrostatic bearing is calculated as follows.

$$Q_{out} = \frac{P_r {h_q}^3}{6\mu}\left(\frac{B - b_1}{l_1} + \frac{L - l_1}{b_1}\right) \tag{6}$$

Where B is the width of the bearing and h_q is the average thickness of the oil sealing surface around the oil chamber. L is the circumferential length between the oil return tanks, the b_1 is the width of the axial sealing oil surface, and the l_1 is the width of the circumferential sealing surface. It can be seen from the law of conservation of mass that the flow rate flowing into the throttle is equal to the flow rate flowing out of the oil chamber, that is, $Q_d = Q_{out}$. Therefore, combining equation (5) and equation (6) can obtain the oil cavity pressure calculation as follows.

$$P_r = \frac{P_s}{1+\beta\left(\frac{h_q}{h_p}\right)^3} \tag{7}$$

Where $\beta = \frac{\ln(r_{d2}/r_{d1})}{\pi}\left(\frac{B-b_1}{l_1} + \frac{L-l_1}{b_1}\right)$, if the spindle is displaced by an external force $f_y(t)$ in the vertical downward direction, the load bearing provided by the hydrostatic bearing w_y as follows

$$w_y = A_e P_s \left(\frac{1}{1+\beta\left(\frac{h_{q3}}{h_{p3}}\right)^3} - \frac{1}{1+\beta\left(\frac{h_{q1}}{h_{p1}}\right)^3} \right) \tag{8}$$

In the formula, $A_e = (B - b_1)(L - l_1)$ is the effective support area of the oil chamber, and the average oil sealing surface thickness around the lower oil cavity and the upper oil cavity is shown below.

$$\begin{cases} h_{q3} = h_0 - y \\ h_{q1} = h_0 + y \end{cases} \tag{9}$$

In equation (8), the throttling gap between the lower oil chamber and the upper oil chamber is as follows

$$\begin{cases} h_{q3} = h_{p0} + \frac{4}{15}(\Delta U - 75) \\ h_{q1} = h_{p0} - \frac{4}{15}(\Delta U + 75) \end{cases} \tag{10}$$

The dynamic balance equation with spindle offset is as follows.

$$M\ddot{y} + B_\xi \dot{y} + f_y(t) + \mathrm{mg} = w_y \tag{11}$$

where B_ξ is the oil film damping coefficient. Combined with the equation (8-11), a simulation model of an active hydrostatic bearing can be obtained.

4. Simulation and analysis

The parameters related to hydrostatic bearings and piezoelectric stacked membrane flow restrictors are shown in Table 2:

Table 2: Parameters of hydrostatic bearings and piezoelectric stacked thin film flow restrictors

parameter	numeric value	parameter	numeric value
Bearing radius r/mm	45	The viscosity of the lubricating oil μ_l/(Pa·s)	3.85×10^{-3}
Bearing width B/mm	90	The density of the lubricating oil ρ_l/(kg/m^3)	810
Return groove spacing L/mm	70	The radius of the oil inlet hole r_{d1}(mm)	1.25
Maximum depth of oil chamber /mm	2	The radius of the throttle table r_{d2}(mm)	8
The width × depth of the oil return tank /mm	3×1.5	Standard throttle gap h_{p0} (um)	60
Radius gap $\boldsymbol{h_0}$/mm	0.025	Oil film damping coefficient B_ξ(N·s/m)	1.3×10^6
Oil supply pressure $\boldsymbol{P_s}$/MPa	2.5	The width of the axial sealing surface b_1/mm	9
Spindle quality M/kg	30	The width of the circumferential sealing surface l_1/mm	8

ISSN 2616-5767 Vol.6, Issue 4: 28-35, DOI: 10.25236/AJETS.2023.060405

4.1. Effect of voltage difference and displacement on bearing capacity

The bearing capacity provided by hydrostatic bearings is w_y nonlinear function, and the above values can be substituted into the equation (8-10), and the relationship between voltage difference, spindle displacement and bearing capacity can be obtained as shown in Figure 4.

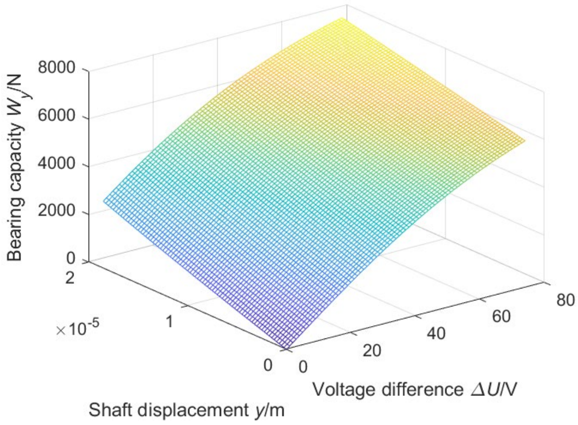

Figure 4: Schematic diagram of the relationship between voltage difference-displacement-bearing capacity

It can be seen from Figure 4 that the bearing capacity of the hydrostatic bearing under the piezoelectric stacked membrane flow restrictor increases approximately equimetrically with the increase of the spindle displacement, and also increases with the increase of the voltage difference of the piezoelectric ceramic stack in the restrictor. Although the voltage difference of the flow limiter is nonlinear with the bearing carrying capacity, it can be fitted to a linear relationship because of the small change in slope.

Linearize equations (8-10) into plane equations as follows:

$$w_y = Ay + B\Delta U + C \tag{12}$$

Planar regression using the regress function in MATLAB is performed as follows.

```
function [A,B,C]=linearization(B,b1,L,l1,h0,Ps,rd1,rd2)
Ae=(B-b1)*(L-l1);By=log(rd2/rd1)/pi*((B-b1)/l1+(L-l1)/b1);
y=zeros(75,75);U=zeros(75,75);pp=zeros(75,75);
for i=1:75
    for j=1:75
    U(i,j)=i-1;y(i,j)=(0.25*10^-6)*(j-1);
    pp(i,j)=Ae*Ps*(1/(1+By*((h0-y(i,j))/((80-0.267*U(i,j))*10^-6))^3)-1/(1+By*((h0+y(i,j))/((80+0.267*U(i,j))*10^-6))^3));
    end
end
a=[U(1,1) U(50,5) U(5,20) …]';
b=[y(1,1) y(50,5) y(5,20) …]';
c=[pp(1,1) pp(5,50) pp(20,5) …]';
scatter3(a,b,c,'filled')
X = [ones(size(a)) a b];
[bb,bint,r ,rint, stats]=regress(c,X);
C=bb(1);A=bb(2);B=bb(3);
```

From this, the linearized fitting plot of voltage difference-displacement-bearing capacity is shown in

ISSN 2616-5767 Vol.6, Issue 4: 28-35, DOI: 10.25236/AJETS.2023.060405

Figure 5.

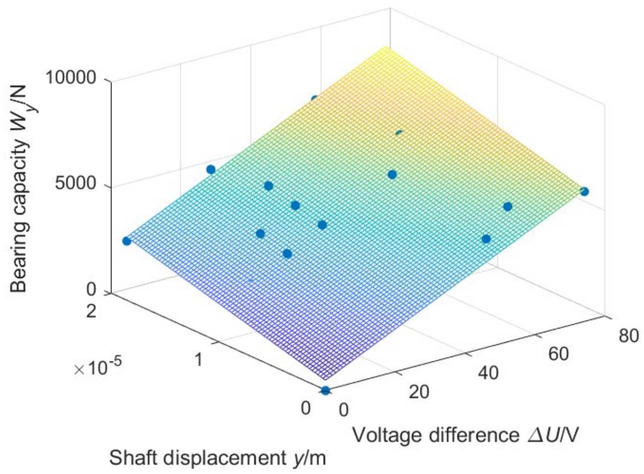

Figure 5: Linearized fit of voltage difference-displacement-bearing capacity

Figure 5 shows that although the fitted bearing capacity is too large when the displacement and voltage difference is too small or too large, when the displacement and voltage difference are moderate, the fitted bearing capacity is small. However, the linearized equation obtained by plane regression by regression function has a good fitting effect on the whole. After obtaining the linearized bearing capacity equation, the control equation can be reduced to a transfer function. Combining (11) and (12) to perform the Larsen transformation yields the following equation.

$$MS^2\mathrm{Y(S)} + B_{\xi}SY(S) + f_y(t) + \mathrm{mg} = AY(S) + B\Delta U + \mathrm{C} \tag{13}$$

This results in a transfer function that looks like this:

$$G(s) = \frac{Bs + \mathrm{C} - f_y(t) - \mathrm{mg}}{MS^2 + B_{\xi}S - A} \tag{14}$$

For this nonlinear transfer function, the PID control algorithm can be directly used to control the displacement sensor in the lower oil cavity, and the iso-oil film control method is used to control the hydrostatic bearing. The system control diagram is shown in Figure 6.

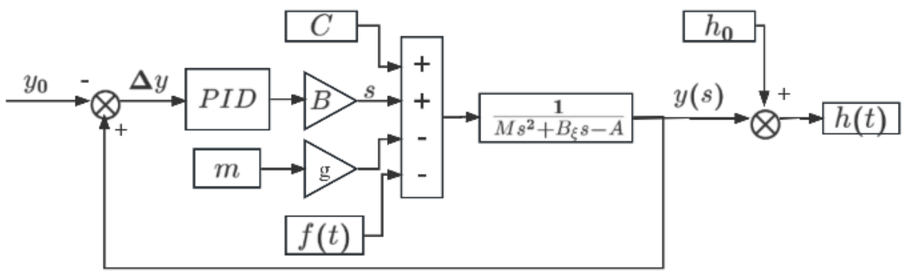

Figure 6: System control schematic

The parameters of the debugged PID are: $K_p = 2.0478, K_i = 119.4673, K_d = 0.0078$.

4.2. Effect of external force on the thickness amplitude of the oil film

In order to reflect the dynamic performance of this control system, the hydrostatic bearings are subjected to external forces $f_y(t)$=2000N, 4000N and 6000N in the vertical direction when *t*=0.1, 0.2 and 0.3s, respectively. The change of oil film thickness at the lower oil cavity of the active hydrostatic bearing under different external forces can be obtained, as shown in Figure 7.

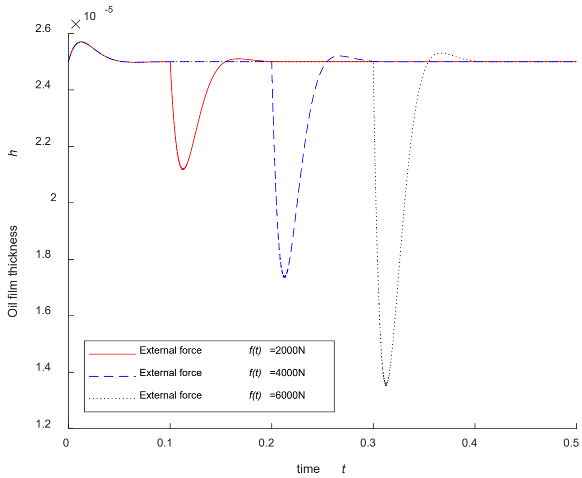

Figure 7: Changes in oil film thickness under different external forces

It can be seen from Figure 7 that under this PID parameter, the oil film thickness has a better control effect. When the time T is close to zero, the oil film thickness of the lower oil chamber first increases and then decreases due to active control, which may be due to the fact that the piezoelectric stacked film throttle compensates too much during initial operation in order to compensate for the oil film thickness of the lower oil chamber caused by the weight of the spindle. When the hydrostatic bearing is subjected to an external force, the oil film thickness amplitude increases linearly with the increase of the external force. Combined with Figure 4 and Figure 5, it can be seen that when the voltage difference ΔU remains zero, the active flow limiter is equivalent to a fixed flow restrictor, and when the voltage difference ΔU increases, the bearing capacity of the hydrostatic bearing is greatly improved. Therefore, compared with fixed flow restrictors, active flow restrictors can greatly increase the bearing capacity and stiffness of hydrostatic bearings.

4.3. Effect of oil supply pressure on the thickness amplitude of the oil film

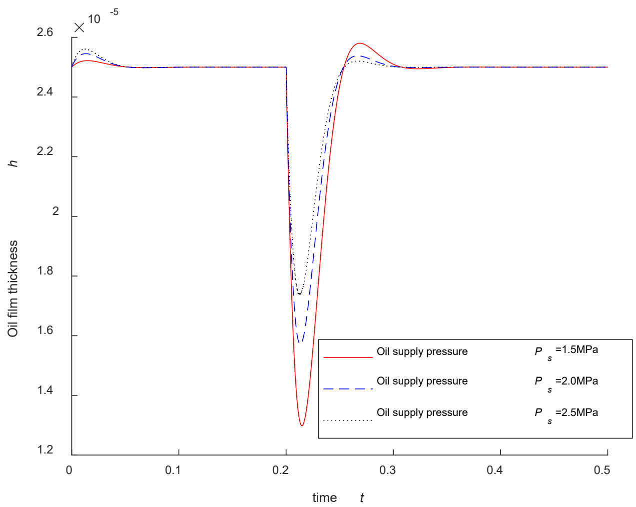

Figure 8: Changes of oil film thickness under different oil supply pressures

In order to test the influence of hydrostatic bearing structure on control, the external force $f_y(t)$=4000N is given to hydrostatic bearings under different oil supply pressures at t=0.2s, and the oil film change diagram under different oil supply pressures can be obtained, as shown in Figure 8, as shown in Figure 8, it can be seen from the figure: under the control of the same PID parameter, the amplitude of the oil film thickness decreases with the increase of the oil supply pressure, but the control response time remains unchanged, the reason may be: under the same external force, the bearing bearing capacity increases with the increase of the oil supply pressure. Therefore, the amplitude of the oil film thickness decreases with the increase of the oil supply pressure. Combined with equation (8), it can be seen that the change of oil supply pressure has no effect on the relationship between the spindle displacement and the voltage difference, so it has no effect on the response time.

Similarly, the increase in bearing width and oil chamber size of hydrostatic bearings can reduce the amplitude of the oil film thickness, but has little effect on the response time of active control.

5. Conclusions

Firstly, based on the piezoelectric equation, flow equation and dynamic balance equation, this paper establishes the control model of active hydrostatic bearings under piezoelectric stacked thin film flow restrictors.

Secondly, through the linearization of the bearing capacity of hydrostatic bearings by the regress function in MATLAB, the control of equal oil film thickness under the PID algorithm is realized, which greatly reduces the computational burden of the control algorithm.

Third, it is found that the increase of oil supply pressure, bearing width and oil cavity size in hydrostatic bearings can reduce the variation of oil film thickness, but has little effect on the response time of active control.

References

[1] Corbett J, McKeown P A, Peggs G N, et al.(2000). Nanotechnology: international developments and emerging products. CIRP Annals, (2), 523-545.

[2] Xiong Wanli, Hou Zhiquan, Lv Lang.(2014). Study on the formation mechanism of rotation error of hydrostatic spindle. Journal of Mechanical Engineering, (07),112-119.

[3] Hu Can, Xiong Wanli, Sun Wenbiao, Yuan Shuai.(2019). Study on the mechanism of improving the rotation accuracy of controlled throttling hydrostatic spindle. Journal of Mechanical Engineering, (11), 160-168.

[4] Woody S, Smith S.(2006). Design and performance of a dual drive system for tip-tilt angular control of a 300 mm diameter mirror. Mechatronics, (7), 389-397.

[5] Kenton B J, Fleming A J, Leang K K.(2011), Compact ultra-fast vertical nanopositioner for improving scanning probe microscope scan speed. Review of Scientific Instruments, (12).

[6] Yang X G, Wang Y Q, Jiang G Y, et al.(2015). Dynamic characteristics of hydrostatic active journal bearing of four oil recesses. Tribology Transactions, (1), 7-17.

[7] Huang Jixiong, Liu Yu, Li Peng.(2017). Simulation analysis of film restrictor for active control of hydrostatic bearing. Combined Machine Tool and Automatic Processing Technology, (02), 65-67+72.

[8] Liu Lei, Liu Baoguo, Wang Pan, Shen Huipeng, Ding Hao, Zheng Jinyong.(2019). Pressure field and temperature field analysis of hydrostatic bearing oil film. Mechanical and Electrical Engineering, (09), 900-906.

[9] Liu Yu.(2017). Design and performance analysis of actively controlled hydrostatic bearing film flow restrictor, Master's thesis, Wuhan University of Technology, Wuhan, Hubei Province.